How does paw pad of Canine attenuate ground impacts: a micromechanical finite element study

Huaibin Miao[1], Jun Fu[1], Zhihui Qian[1*], Luquan Ren[1], Lei Ren[1, 2]

[1]Key Laboratory of Bionic Engineering, Jilin University, Changchun, 130022, P.R. China
[2]School of Mechanical, Aerospace and Civil Engineering, University of Manchester, Manchester, M13 9PL, United Kingdom

Corresponding Author:

Dr. Zhihui Qian
Key Laboratory of Bionic Engineering
Jilin University
Changchun
130022, P.R. China
Tel: +86 431 85095760
Email: zhqian@jlu.edu.cn

Keywords: paw pad, micro-structure, finite element, cushioning, off-loading

Word count (introduction through conclusion): 3760

Submitted as: Original research article

(Submitted to PeerJ)

Abstract

Background. Digitigraded mammals, e.g. dogs and cats, stand or walk on their digits or toes. Their paw pads beneath the digits or toes, rather than the entire sole of the foot, are in contact with the ground surface during locomotion. Digitigrades generally move more quickly and quietly than other animals. So far, little is known about the micro-scale structural characteristics of digitigrades' paw pads and its connection with the superior biomechanical functioning of their feet.

Methods. In this study, we investigated the micro-structure of the paw pad of German shepherd dog (GSD) using SEM and histological examination, and assessed the biomechanical functions of the micro-structured epidermis layer by using dynamic finite element (FE) simulations.

Results. We found that there exists a thick layer of stratified epithelium of a honeycomb like structure with conical protuberances (i.e. dermal papilla) embedded in each cell unit. Our FE simulation analyses revealed that this specially structured layer is capable of effectively attenuating the ground impact across a range of impact velocities. Moreover, this cushioning capacity becomes more pronounced with increased impact velocity. More importantly, this layer can also significantly reduce the mechanical stress transmitting to the soft dermal papillae and dermis by using an off-loading mechanism.

Discussion. This would provide more insights into the biomechanical functioning of

digitigrade's paw pads, and also facilitate the development of bio-inspired ground contacting components of robots and machines, and also the design of footwear and orthotics devices.

Introduction

For land mammals, the foot is normally the first part of the body to touch the ground surface at each step during locomotion, which is cyclically subjected to large transient ground reaction force (GRF) that may reach as high as two or three times the body weight due to the interaction between the foot and the ground (Jayes & Alexander, 1978; Bryant et al., 1987; Budsberg, Verstraete & Soutas, 1987; Budsberg et al., 1995). A shock wave caused by GRF usually transmits along the animal body and reaches to the skull. The GRF and the shock wave have been suggested as the primary etiological agents in degenerative joint diseases and injuries of the musculoskeletal system (Collins & Whittle, 1989; Whittle, 1999; Gill & O’Connor, 2003a; Gill & O’Connor, 2003b; Chi & Schmitt, 2005). As the only body part in contact with the ground during locomotion, the feet of land mammals play a critical role in attenuating and transmitting GRF effectively to minimise potential damages of the musculoskeletal system (Jahss, Kummer & Michelson, 1992).

The feet of digitigrade mammals, e.g. dogs and cats, are anatomically different from those plantigrades or unguligrades (Boyd et al., 1995). Digitigrades have relatively long carpals and tarsals, and stand or walk on their digits or toes. Their paw pads beneath the digits or toes, rather than the entire sole of the foot, are in contact with the ground surface during locomotion. The soft tissues of paw pads of digitigrades may be more prone to tissue injuries (Gustås et al., 2004; Warner et al., 2013). Additionally, digitigrades generally move more quickly and quietly than other animals. So, their paw pads may have superior capabilities to attenuate ground impacts and absorb kinetic energy.

Over the past decades, a large number of studies have been conducted to investigate the biomechanics of the footpads of land mammals (Alexander, Bennett & Ker, 1986; Ker, 1999; Weissengruber et al., 2006; Ledoux & Blevins 2007; Chi & Roth 2010; Natali, Fontanella & Carniel, 2010; Qian, Ren & Ren, 2010; Fontanella et al., 2013). However, most of those investigations were focused on the mechanical behaviour of heel pads of plantigrades, e.g. humans (Natali, Fontanella & Carniel, 2010; Qian, Ren & Ren, 2010; Fontanella et al., 2013). Very few studies have been performed to study the biomechanical behaviour of the paw pads of digitigrades. Alexander et al. examined the bulk viscoelastic material properties of paw pads of some mammals, and found they are similar to those of heel pads, which may contribute to moderating ground impact and preventing from chattering (Alexander, Bennett & Ker, 1986). A recent study found that the structural properties of the animal's footpa unlike other biological supporting structures, scale interspecifically by changing both geometry and material properties in order to maintain and operate the musculoskeletal locomotor system (Ledoux & Blevins, 2007). Indeed, a good understanding of the mechanical design principle of animal's footpads may advance the design of ground contacting components of legged robots, machines or healthcare products, e.g. footwear insoles and bases. However, so far little is known about the structural characteristics of digitigrades' paw pads at micro level and its connection with the foot biomechanical functioning.

The objective of this study is to investigate the mechanical and structural characteristics of digitigrades' paw pads at micro level using German shepherd dog (GSD) as an example model. GSD is one of the most popular breeds of dog around the world, and is preferred for many types of work, including disability assistance, search-and-rescue, police and military roles because of their strength, locomotor capability and intelligence. Histological examination of paw pad tissues was conducted using tissue staining and scanning electron microscopy (SEM) methods. Micromechanical analysis based on finite element (FE) method was used to investigate the effect of micro-structure on biomechanical functioning. We hypothesize that the paw pad of digitigrades has multi-layer micro-structure as the heel pad of plantigrades, and this multi-layer structure contributes to the superior cushioning capacity and also structural integrity of the paw pads.

Materials & Methods

Ethical statement

This study was conducted with the approval of the Institutional Review Board Committee of Jilin University, Changchun, P.R. China (NO. 20140418).

Histological examination

Two adult cadaver GSDs were donated for this study by the police dog training base of the Public Security Bureau of Jilin Province in Changchun City. They died of an accident during training and were immediately frozen and stored for four weeks before transporting to our lab at Jilin University. Both dogs do not have any recorded histories of musculoskeletal disorders or diseases, and their feet are in healthy intact condition. Their forefeet were amputated, and the tissue samples of the metacarpal pads were prepared by the Animal Experiment Centre of Bethune School of Medicine at Jilin University. The metacarpal pad specimens were cut into ten 5-µm-thick slices in the sagittal plane and transverse plane and two cubes of approximately 8mm×8mm×8mm and two cuboids of approximately 8mm×8mm×3mm. The samples were then placed in l0% neutral buffered formalin for 48 hours, and thereafter were embedded in paraffin and dehydrated for 3 hours at 60°C. The 5-µm-thick slices were stai with haematoxylin and eosin, and also Masson's trichrome stain for histological examination. The cubes and cuboids were washed in distilled water and then air dried. All the samples were mounted on aluminium stubs and coated with gold palladium for observations (the cubes were observed in the sagittal plane and the cuboids were observed in the transverse plane) with a scanning electron microscope (EVO 18, Carl Zeiss Microscopy GmbH, Jena, Germany).

Finite element modeling

Based on the footpad micro-structure found by the SEM and histological examinations (see figures 2 and 3 in the Results section for details), a micromechanical FE model of the epidermis layer of the paw pad was constructed to investigate the biomechanical function of the footpad layer. The model consists of stratified epithelium structure and embedded dermal papillae (see figure 1). To simplify the modelling, only 1% portion of the layer was constructed by using cylinders to represent dermal papillae (see figure 1B and 1C). A rectangular plate was firmly connected to the top surface of the layer to represent the corresponding effective mass (Qian, Ren & Ren, 2010). Another fixed rectangle plate beneath the tissue layer was used to simulate the ground surface. The three-dimensional (3D) geometry of the layer and plates was created using Solidworks software (Dassault Systèmes Corp., Waltham, U.S.A.). Those geometric parts were then imported into and assembled in the FE modelling software ABAQUS (Dassault Systèmes Corp., Waltham, U.S.A.).

PeerJ Preprints | https://doi.org/10.7287/peerj.preprints.2340v1 | CC BY 4.0 Open Access | rec: 4 Aug 2016, publ: 4 Aug 2016

tetrahedral elements were used for the mesh generation of the stratified epithelium structure and the papillae, and hexahedral elements were used for the two plates. In total, 26266 elements were used for the whole model construction (see figure 1A).

In this study, the stratified epithelium and dermal papillae were considered as homogeneous, isotropic and linear elastic materials (Luboz et al., 2014). Their material properties were defined based previous literature data (Cheung et al., 2005; Luboz et al., 2014). To simplify, the top and bottom plates were modelled as rigid bodies. The material properties and the element types of each part of the model were listed in Table 1. The dermal papillae were considered as being firmly embedded in the stratified epithelium structure without relative motions. Whereas the footpad-ground interface was defined as a contact surface with a frictional coefficient of 0.6 (Cheung et al., 2005). The top plate representing the effective mass of the layer portion has a mass of 0.11kg, which was estimated from the mass of a representative cadaver dog and also the percentage of the layer portion.

Dynamic simulation analyses

In this study, dynamic FE simulations were conducted to analyse the biomechancial function of the structured epidermis layer in stance phase of locomotion. The top plate, together with the stratified epithelium and the dermal papillae, was defined to contact the ground pl vertically with an initial velocity in the range from 1mm/s to 35mm/s, which was estimated from the metacarpal marker data in the stance phase of normal walking of GSDs (Qian et al., 2014). The dynamic responses of the vertical GRF and also the vertical displacement of the top plate were simulated at eight different impact velocities: 1mm/s, 2mm/s, 4mm/s, 6mm/s, 10mm/s, 20mm/s, 30mm/s, 35mm/s.

To investigate the effect of the structured epidermis layer on the biomechanical functioning, an uniform model was also constructed by assuming that the entire layer is composed of the same homogeneous, isotropic and linear elastic material as that of the stratified epithelium. The same dynamic FE simulation cases were also conducted for the uniform model by using the same loading and boundary conditions as those for the structured model. In addition, material property sensitivity analyses were also performed to examine the effect of the Young's modulus of the dermal papillae on the footpad functioning by changing the elastic modulus of the dermal papilla to 0.0004MPa, 0.04MPa, 0.4MPa and 4MPa respectively from the baseline value of 0.004MPa.

Results

The scanning electron microscope (SEM) and histological examination results of the paw pad samples of a representative dog are shown in Figure 2−4. We can see that the bottom surface of the paw pad, which was in direct contact with the ground surface during locomotion, is covered by a layer of spike-like stratum corneum (see figure 2A and 3A). Above that is a thick layer of stratified epithelium of a honeycomb like structure with conical protuberances (i.e. dermal papilla) embedded in each cell unit (see figure 2A and 2B). The dermal papillae are composed of matrix tissues and are basically the small protrusions of the dermis projecting into the honeycomb cells of the stratified epithelium (see figure 3A and 3B). Interestingly, we found that this kind of honeycomb structure only exits in the bottom epidermis layer of the paw pad in contact with the ground surface during locomotion. The epidermis of the other parts of the footpad, e.g. the layer by the side wall, doesn't show the structured honeycomb pattern (see figure 4). Further up superiorly is the dermis layer lying adjacent to the stratified epithelium and dermal papillae. In the middle of the dermis layer, reticulated layer of bundles of collagen fibers with few interspersed elastic fibers are distributed (see figure 3C). Above the dermis layer lies the subcutaneous layer constraining a large amount of subcutaneous adipose tissues (see figure 3A), which are separated by collagenous membranes into many small compartments (see figure 3D).

PeerJ Preprints | https://doi.org/10.7287/peerj.preprints.2340v1 | CC BY 4.0 Open Access | rec: 4 Aug 2016, publ: 4 Aug 2016

To investigate the mechanical functioning of the characteristic honeycomb structured epidermis layer, dynamic FE simulations were conducted at eight different initial loading velocities using both the structured model (consisting of the dermal papillae and the stratified epithelium) and the uniform model (see details in Materials and Methods section). Figure 5 shows the simulated vertical GRFs and the vertical displacements of the top plate by both models under a loading velocity of 30 mm/s. We can see that the GRFs and vertical displacements show typical single-hump patterns associated with a loading and unloading cycle. From Figure 5A, it can be seen that the structured epidermis layer significantly lowers the peak vertical GRF acting on the paw pad leading to a 35% drop in peak force from 1.3N to 0.85N in contrast to the uniform model. Whereas the peak vertical displacement of the top mass is increased by about 38% in the structured model (see figure 5B).

Figure 6 shows the simulated von Mises stress distributions in the footpad sample by both models under the peak vertical GRFs. The uniform model presents much higher maximum von Mises stress (3.157MPa) than that of the structured model (2.455MPa) probably because of the stress concentrate in the ground contact area. We can also see that the von Mises stresses on the top surface of the structured model (around 10^{-6}MPa) are much lower than those in the uniform model (around 10^{-3}MPa). In the structured model, the von Mises stress drops dramatically along the longitudinal axis of the dermal papillae from bottom to top (

the four white nodes in figure 6A with von Mises stresses of 0.976, 0.0005, 0.0002, 0.0001MPa respectively in a bottom-up order). Whereas in the uniform model, higher von Mises stresses are shown at the same nodes along the longitudinal axis also with a bottom-up decreasing pattern (see the four white nodes in figure 6B with von Mises stresses of 1.04, 0.389, 0.225 and 0.065MPa respectively in a bottom-up order). However, the stress decreases much more gently than in the structured model. Interestingly, an opposite trend is found in the simulated stresses in the stratified epithelium. The structured model predicts higher von Mises stresses than the uniform model at the same nodes (see the three red nodes in figure 6A with von Mises stresses of 0.472, 0.408, 0.305MPa respectively in a bottom-up order, and the corresponding red nodes in Figure 6B with von Mises stresses of 0.284, 0.25, 0.135MPa respectively from bottom to top). The bottom-up decreasing pattern in stress along the longitudinal direction also presents for both models in the stratified epithelium. However, the stress decreasing grade of the structured model is lower than that of the uniform model.

Figure 7A shows the predicted peak vertical GRFs acting on the footpad by both models at eight different initial impact velocities. We can see that the peak GRFs increase with increased impact velocity in both models, and the increasing slope of the uniform model is greater than that of the structured model. The ratios of the peak GRFs predicted by the structured model over those by the uniform model at different impact velocities are shown

Figure 7B. It can be seen that the peak GRF ratio decreases rapidly with increased impact velocity indicating that greater cushioning capacity is provided by the honeycomb structured epidermis layer at higher impact velocity.

Figure 7C shows the simulated peak vertical displacements at the top plates by both models and Figure 7D also shows the peak displacement ratios between the two models at different impact velocities. It can be seen that the peak vertical displacement increases with increased impact velocity in both models, and higher peak displacement is generated by the structured model. Similarly, the maximum von Mises stresses predicted by both models and also the stress ratios between the two models at different impact velocities are shown in Figure 7E and Figure 7F. We can see that the maximum von Mises stresses generally increase with increased impact velocity in both models, and the structured model generates lower stresses than the uniform model especially at impact velocity higher than 10 mm/s.

Figure 8 shows the results of the material property sensitivity analysis investigating the effect of the Yong's modulus of the dermal papilla on the peak vertical GRFs and the peak vertical displacements at the top plate at different impact velocities. We can see that the peak vertical GRFs and the vertical displacements almost increase linearly with increased impact velocity. Softer dermal papilla material leads to lower slope in the peak vertical GRF curve, but resu in higher gradient in the peak vertical displacement curve. This indicates that decreasing the Yong's modulus of the dermal papilla would greatly attenuate the peak vertical GRF especially at higher impact velocities. However, there is a plateau in this cushioning capacity increase. When the Yong's modulus of the dermal papilla is lower than a critical value of 0.04-0.004MPa, the slopes of both peak vertical GRF and peak vertical displacement curves will stop increasing with decreased Yong's modulus. In this scenario, the cushioning function of the footpad reaches a maximum capacity.

Discussions

Our SEM and histological examination results suggest that the paw pad of GSD consists of three layers: the outmost stratum corneum, intermediate epidermis and dermis layer and also the subcutaneous layer. The bottom part of the stratum corneum is in direct contact with the ground surface during locomotion, and is composed of the hardest material (Young's modulus E ≈ 6MPa, Luboz et al., 2014) among all the three layers presumably to endure the tremendous pad-ground wear, friction and impact during locomotion (Meyer et al., 1990; Luboz et al., 2014). The subcutaneous layer consists of adipose tissue, which are basically adipocytes filled with lipids. They are separated by collagenous membranes into many small compartments. Similar structures were also found in the subcutaneous layer of the footpads human beings and other animals, e.g. elephants and leopards (Alexander, Bennett & Ker, 1986; Weissengruber et al., 2006; Hubbard et al., 2009; Qian, Ren & Ren, 2010; Mihai, Alayyash & Goriely, 2015). The mechanical behaviour of adipose tissue was normally considered as equivalent to a hydrostatic system filled up with incompressible fluid (Pond, 1998; Ker, 1999; Chi & Roth, 2010). Indeed, the subcutaneous layer is formed by the softest material (Young's modulus E ≈ 0.001MPa, Luboz et al., 2014) among all the three layers, and is the foremost energy absorber of footpads (Ker, 1999; Weissengruber et al., 2006). The epidermis and dermis layer lies in between the hardest and softest layers of the footpad, of which the Young's modulus has about 6000 times difference. So far, little is known about its biomechanical functioning during locomotion. In this study, we found that in the footpad of GSD, the bottom part of the epidermis layer has a distinctive honeycomb structure at microscale level consisting of stratified epithelium and dermal papillae. Our dynamic FE analyses reveal that this specially micro-structured layer may provide multiple biomechanical functionalities.

Cushioning is one of the most important biomechanical functions of animal's feet. Our FE simulation results showed that the structured epidermis layer is capable of attenuating the peak GRF across a range of impact velocity much more effectively than a uniform epithelium layer. This is expected as the dermal papillae filled in the cell units of the honeyco structure is much softer than the epithelium tissue. Interestingly, this structured epidermis layer brings in a favourable mechanical characteristic to the footpad enabling stronger cushioning capacity at higher impact velocity. This property is highly desirable for the locomotor system because our simulation results suggest that the peak GRF almost increase linearly with increasing impact velocity. Because both the stratified epithelium and the dermal papillae are modelled as linear elastic rather than viscoelastic materials in this study, this helpful velocity-dependent feature is very likely due to the honeycomb structure at the microscale level. Moreover, the material property sensitivity analysis suggests that the increasing cushioning capacity of the epidermis layer plateaus after the Young's modulus of the dermal papillae is lower than 0.04-0.004MPa. Indeed, this honeycomb micro-structures consisting of stratified epithelium and dermal papillae was also found in the paw pads of other digitigrade mammals, such as cats and leopards (Hubbard et al., 2009; Ninomiya et al., 2011), suggesting that this characteristic structure may be desirable for their quieter and faster locomotion patterns.

The moderated GRF due to the cushioning function could lead to low mechanical stresses in the footpad tissues. This is supported by our FE simulation results, which show that the peak von Mises stress in the epidermis layer is noticeably lowered by the honeycomb micro-structure especially at higher impact velocities. This agrees with the suggestion by a previ experimental study that a honeycomb structure is advantageous as being a shock absorber during impact (Yamashita & Gotoh, 2005; Burlayenko & Sadowski, 2010; Qian, Ren & Ren, 2010). However, a closer examination of the stress distributions predicted by our FE models in the whole epidermis layer reveals that only the stress in the dermal papillae is decreased, whereas higher stress is found in the stratified epithelium due to the honeycomb structure. It appears that the structured layer provides an offloading mechanism by transferring load to the hard stratified epithelium whilst reducing the stress in the soft dermal papillae. This leads to significantly lowered von Mises stress at the top surface of the epidermis layer (around 10^{-6}MPa), which is almost 1000 times lower than that of an uniform layer. It's evident that the honeycomb micro-structure consisting the hard stratified epithelium and the soft dermal papillae provides an excellent offloading function to protect the soft materials in the dermis and subcutaneous layers, and hence to maintain the structural integrity of the footpad.

In addition to the lowered GRF and tissue stress, the structured epidermis layer also results in increased vertical displacement, due to the soft dermal papillae embedded in the cell units, showing an rising tendency with increased impact velocity. This is generally undesirable because large vertical displacement may lead to long stance duration and low moving speed during locomotion. Moreover, it may also worsen the lateral stability of stance feet. In this study, the stratified epithelium and the dermal papillae were considered as linear elas

PeerJ Preprints | https://doi.org/10.7287/peerj.preprints.2340v1 | CC BY 4.0 Open Access | rec: 4 Aug 2016, publ: 4 Aug 2016

materials in the modelling. However, biological materials are non-linear and viscoelastic in nature. The viscous effect and the increased Young's modulus due to the material non-linearity would help to attenuate the vertical displacement when the impact velocity increases. Moreover, the vertical displacement would be further damped by the subcutaneous layer, which consists of adipose tissue and acts as a hydrostatic system (Pond, 1998; Ker, 1999; Chi & Roth 2010). Indeed, all the three layers in the paw pad work as a whole to meet the biomechanical requirements of animal locomotion. The tough stratum corneum layer sustains the harsh ground-pad interactions. The intermediate epidermis and dermis layer weakens the ground impact and offloads the high tissue stress. The large bulk of adipose tissue in the subcutaneous layer further moderates the ground impact and tissue displacement by absorbing the impact energy. Finally, all the envelope interfaces between layers together ensure the structural integrity of the whole pad system.

Conclusions

We investigated the micro-structure of the paw pad of GSDs using SEM and histological examination, and assessed the biomechanical functions of the honeycomb structured epidermis layer by using dynamic FE analyses. It was found that this specially structured layer is capable of effectively attenuating the ground impact across a range of impact veloc

More importantly, it can significantly reduce the mechanical stress acting on the dermal papillae and dermis by using an off-loading mechanism. This would provide more insights into the biomechanical functioning of the digitigrade's paw pads, and also facilitate the development of bio-inspired ground contacting components of robots and machines, and also the design of footwear and orthotics devices. Dogs are well adapted to cold climates. A recent study suggested the structured epidermis layer may provide a heat conserving mechanism as well (Ninomiya et al., 2011). It is worth a further investigation to understand how this honeycomb micro-structured layer achieves multiple physical functionalities in impact attenuation, stress off-loading and heat conservation simultaneously.

Competing interests

We declare we have no competing interests.

Funding

This work was supported by the project of National Natural Science Foundation of China (No.51105167 & 51475202), the scientific and technological development planning project of Jilin Province (No.20130522187JH) and the China Postdoctoral Science Foundation func project (No. 2014T70293 & 2013M530985).

References

Alexander R, Bennett M, Ker R. 1986. Mechanical properties and function of the paw pads of some mammals. *Journal of Zoology* 209:405-419. DOI: 10.1111/j.1469-7998.1986.tb03601.x

Boyd JS, Paterson C, Schnorr M, Schnorr B. 1995. *A colour atlas of clinical anatomy of the dog and cat:* Ferdinand Enke Verlag.

Bryant J, Bennett M, Brust J, Alexander R. 1987. Forces exerted on the ground by galloping dogs (Canis familiaris). *Journal of Zoology* 213:193-203. DOI: 10.1111/j.1469-7998.1987.tb03693.x

Budsberg SC, Verstraete MC, Brown J, Reece L. 1995. Vertical loading rates in clinically normal dogs at a trot. *American journal of veterinary research* 56:1275-1280.

Budsberg SC, Verstraete MC, Soutas-Little RW. 1987. Force plate analysis of the walking gait in healthy dogs. *American journal of veterinary research* 48:915-918.

Burlayenko V, Sadowski T. 2010. Effective elastic properties of foam-filled honeycomb cores of sandwich panels. *Composite Structures* 92:2890-2900. DOI: 10.1016/j.compstruct.2010.04.015

Cheung JT-M, Zhang M, Leung AK-L, Fan Y-B. 2005. Three-dimensional finite element analysis of the foot during standing—a material sensitivity study. *Journal of Biomechanics* 38:1045-1054. DOI: 10.1016/j.jbiomech.2004.05.035

Chi K-J, Roth VL. 2010. Scaling and mechanics of carnivoran footpads reveal the principles of footpad design. *Journal of The Royal Society Interface* 7:1145-1155.

DOI: 10.1098/rsif.2009.0556

Chi K-J, Schmitt D. 2005. Mechanical energy and effective foot mass during impact loading of walking and running. *Journal of Biomechanics* 38:1387-1395. DOI: 10.1016/j.jbiomech.2004.06.020

Collins J, Whittle M. 1989. Impulsive forces during walking and their clinical implications. *Clinical Biomechanics* 4:179-187. DOI: 10.1016/0268-0033(89)90023-5

Fontanella C, Forestiero A, Carniel E, Natali A. 2013. Analysis of heel pad tissues mechanics at the heel strike in bare and shod conditions. *Medical Engineering & Physics* 35:441-447. DOI: 10.1016/j.medengphy.2012.06.008

Gill H, O'Connor J. 2003. Heelstrike and the pathomechanics of osteoarthrosis: a pilot gait study. *Journal of Biomechanics* 36:1625-1631. DOI: 10.1016/S0021-9290(03)00189-1

Gill H, O'Connor J. 2003. Heelstrike and the pathomechanics of osteoarthrosis: a simulation study. *Journal of Biomechanics* 36:1617-1624. DOI: 10.1016/S0021-9290(03)00190-8

Gustås P, Johnston C, Roepstorff L, Drevemo S, Lanshammar H. 2004. Relationships between fore‐ and hindlimb ground reaction force and hoof deceleration patterns in trotting horses. *Equine veterinary journal* 36:737-742. DOI: 10.2746/0425164044848136

Hubbard C, Naples V, Ross E, Carlon B. 2009. Comparative analysis of paw pad structure in the clouded leopard (Neofelis nebulosa) and domestic cat (Felis catus). *The Anatomical Record* 292:1213-1228. DOI: 10.1002/ar.20930

Jahss MH, Kummer F, Michelson JD. 1992. Investigations into the fat pads of the sole of the foot: heel pressure studies. *Foot & Ankle International* 13:227-232. DOI: 10.1177/107110079201300501

Jayes A, Alexander R. 1978. Mechanics of locomotion of dogs (Canis familiaris) and sheep

(Ovis aries). *Journal of Zoology* 185:289-308. DOI: 10.1111/j.1469-7998.1978.tb03334.x

Ker RF. 1999. The design of soft collagenous load-bearing tissues. *Journal of Experimental Biology* 202:3315-3324.

Ledoux WR, Blevins JJ. 2007. The compressive material properties of the plantar soft tissue. *Journal of biomechanics* 40:2975-2981. DOI: 10.1016/j.jbiomech.2007.02.009

Luboz V, Perrier A, Stavness I, Lloyd J, Bucki M, Cannard F, Diot B, Vuillerme N, Payan Y. 2014. Foot ulcer prevention using biomechanical modelling. *Computer Methods in Biomechanics and Biomedical Engineering: Imaging & Visualization* 2:189-196. DOI: 10.1080/21681163.2013.837410

Meyer W, Bartels T, Tsukise A, Neurand K. 1990. Histochemical aspects of stratum corneum function in the feline foot pad. *Archives of dermatological research* 281:541-543.

Mihai LA, Alayyash K, Goriely A. 2015. Paws, pads and plants: the enhanced elasticity of cell-filled load-bearing structures. *Proceedings of the Royal Society of London A: Mathematical, Physical and Engineering Sciences: The Royal Society*. p 20150107. DOI: 10.1098/rspa.2015.0107

Natali A, Fontanella C, Carniel E. 2010. Constitutive formulation and analysis of heel pad tissues mechanics. *Medical Engineering & Physics* 32:516-522. DOI: 10.1016/j.medengphy.2010.02.018

Ninomiya H, Akiyama E, Simazaki K, Oguri A, Jitsumoto M, Fukuyama T. 2011. Functional anatomy of the footpad vasculature of dogs: scanning electron microscopy of vascular corrosion casts. *Veterinary Dermatology* 22:475-481. DOI: 10.1111/j.1365-3164.2011.00976.x

Pond CM. 1998. *The fats of life:* Cambridge University Press.

Qian Z, Miao H, Shang Z, Ren L. 2014 The foot-ground contact analysis of german shephe dog based on normal walking, trotting and jumping gait. *Journal of Jilin University*

(Engineering and Technology Edition) 44:1692-1697.

Qian Z, Ren L, Ren L. 2010. A coupling analysis of the biomechanical functions of human foot complex during locomotion. *Journal of Bionic Engineering* 7:S150-S157. DOI: 10.1016/S1672-6529(09)60229-8

Warner SE, Pickering P, Panagiotopoulou O, Pfau T, Ren L, Hutchinson JR. 2013. Size-related changes in foot impact mechanics in hoofed mammals. *PLoS One* 8:e54784 . DOI: 10.1371/journal.pone.0054784

Weissengruber G, Egger G, Hutchinson J, Groenewald HB, Elsässer L, Famini D, Forstenpointner G. 2006. The structure of the cushions in the feet of African elephants (Loxodonta africana). *Journal of Anatomy* 209:781-792. DOI: 10.1111/j.1469-7580.2006.00648.x

Whittle MW. 1999. Generation and attenuation of transient impulsive forces beneath the foot: a review. *Gait & posture* 10:264-275. DOI: 10.1016/S0966-6362(99)00041-7

Yamashita M, Gotoh M. 2005. Impact behavior of honeycomb structures with various cell specifications—numerical simulation and experiment. *International Journal of Impact Engineering* 32:618-630. DOI: 10.1016/j.ijimpeng.2004.09.001

Figures

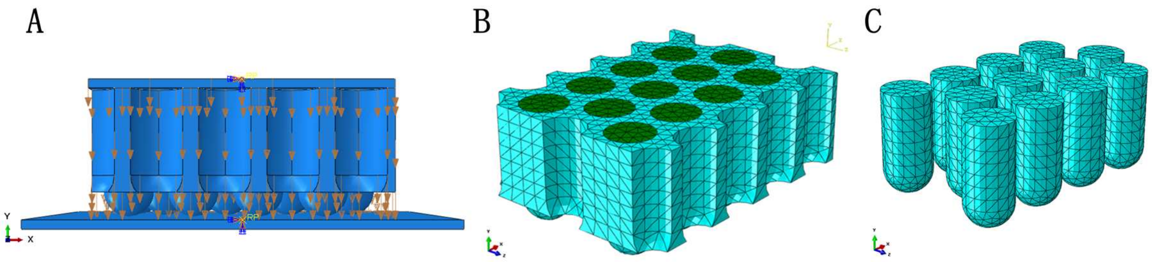

Figure 1

PeerJ Preprints | https://doi.org/10.7287/peerj.preprints.2340v1 | CC BY 4.0 Open Access | rec: 4 Aug 2016, publ: 4 Aug 2016

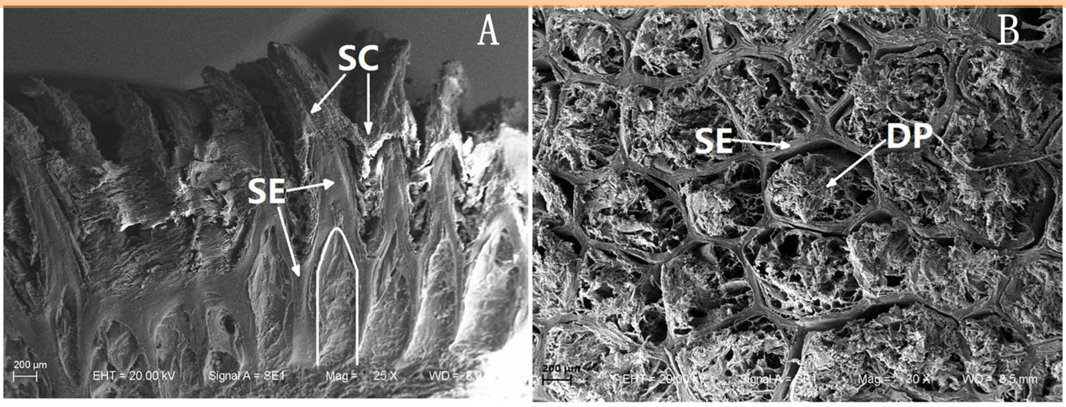

Figure 2

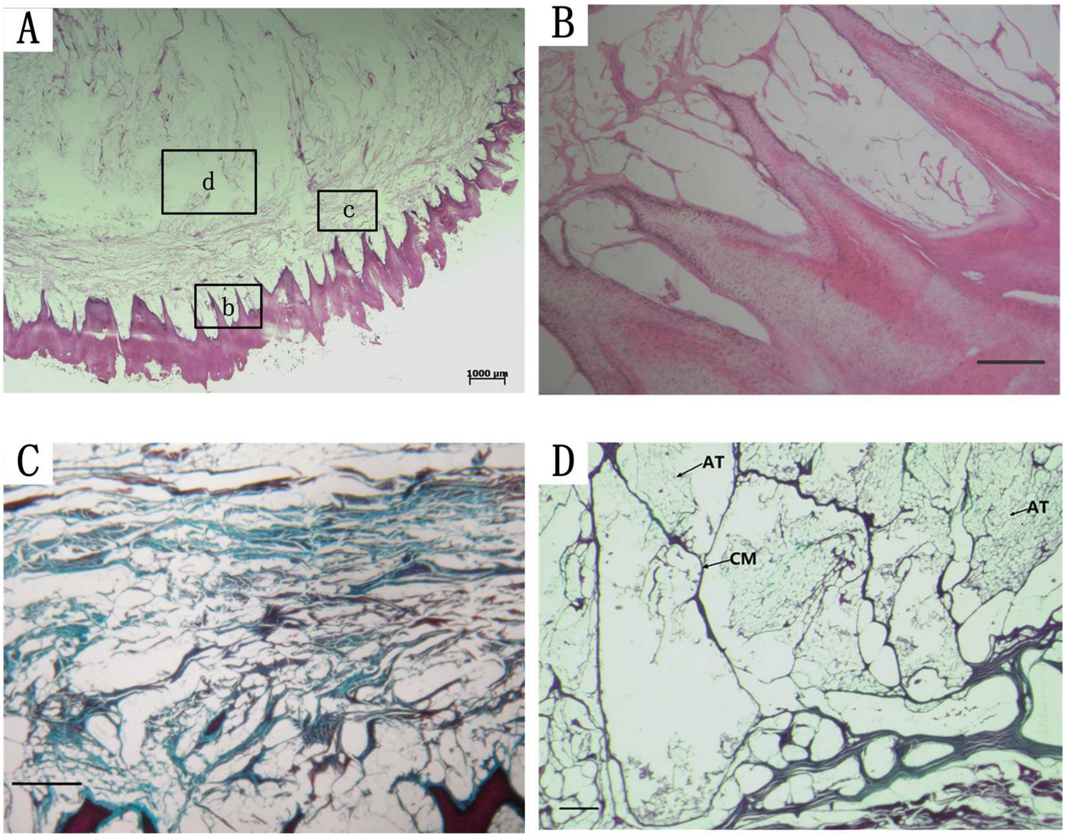

Figure 3

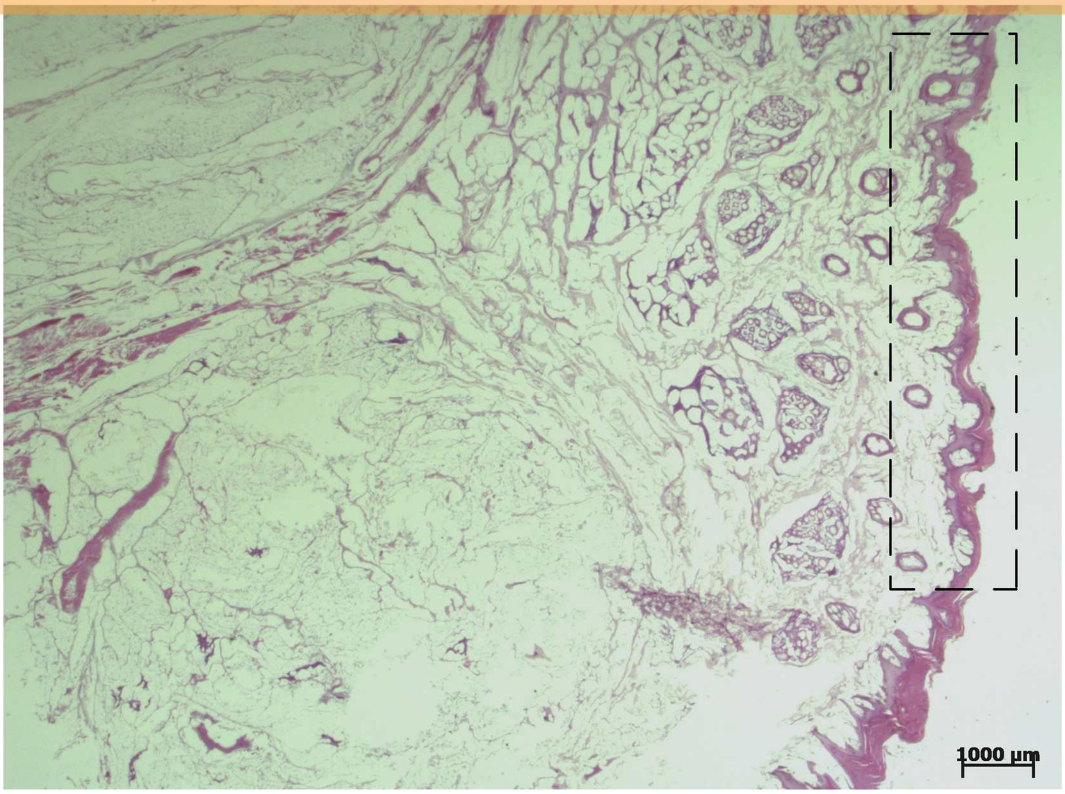

Figure 4

Figure 5

PeerJ Preprints | https://doi.org/10.7287/peerj.preprints.2340v1 | CC BY 4.0 Open Access | rec: 4 Aug 2016, publ: 4 Aug 2016

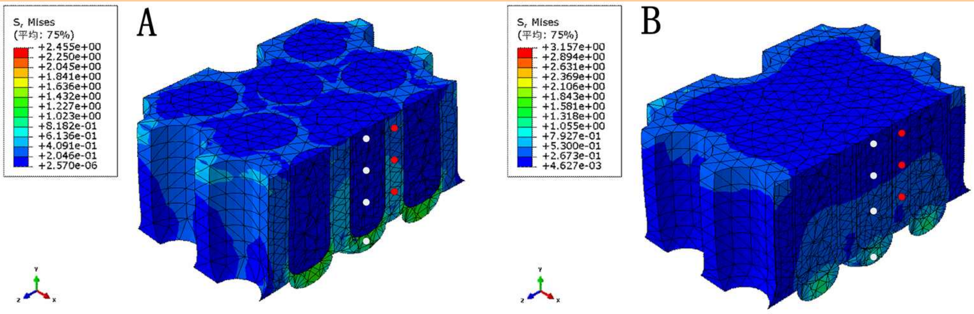
S, Mises
(平均: 75%)
+2.455e+00
+2.250e+00
+2.045e+00
+1.841e+00
+1.636e+00
+1.432e+00
+1.227e+00
+1.023e+00
+8.182e-01
+6.136e-01
+4.091e-01
+2.046e-01
+2.570e-06
A
S, Mises
(平均: 75%)
+3.157e+00
+2.894e+00
+2.631e+00
+2.369e+00
+2.106e+00
+1.843e+00
+1.581e+00
+1.318e+00
+1.055e+00
+7.927e-01
+5.300e-01
+2.673e-01
+4.627e-03
B

Figure 6

Figure 7

Figure 8

Figure Captions

Figure 1 The micro-scale finite element model of 1% portion of the paw pad of a representative GSD. (A) Assembly model with the top plate and the ground surface. Yellow arrows represent the direction of the impact velocity. (B) Model of the stratified epithelium with embedded dermal papillae. (C) Model of the dermal papillae.

Figure 2 Scanning electron microscope image of the stratified epithelium. (A) Sagittal section of the stratified epithelium. White line represents the profile of honeycomb crust. (B) Transverse section of the stratified epithelium. Abbreviations: SC, stratum corneum; SE, stratified epithelium; DP, dermal papillae.

Figure 3 Histology of the paw pad of a representative GSD. (A) The whole mount of the paw pad. (B) Stratified epithelium and dermal papillae. (C) Dermis layer. Collagen fibers are in blue. (D) Collagenous membranes and adipose tissue distributed in the subcutaneous adipose tissue. Abbreviations: CM, collagenous membrane; AT, adipose tissue. (A) and (B) were stained with hemotoxylin and eosin; (C) and (D) were stained with Masson. Scale bars in (B), (C) and (D) represent 200μm.

Figure 4 Transverse section near the side wall of the paw pad. The boxed area is the side wall of the footpad that is not in direct contact with the ground surface.

Figure 5 The predicted time histories of the vertical GRF (A) and the displacements of the top plates (B) by both the uniform model and the structured model.

Figure 6 The simulated von Mises stress distribution under peak GRFs at the impact velocity 30mm/s by structured model (A) and uniform model (B).

Figure 7 The peak vertical GRFs (A), the peak vertical displacements (C) and the peak von Mises stresses (E) predicted by the structured and uniform models at different impact velocities; and the peak vertical GRF ratio (B), the peak vertical displacement ratio (D) and the peak von Mises stress ratio (F) between the structured model and the uniform model across different impact velocities.

Figure 8 The simulated peak vertical GRFs (A) and peak vertical displacements (B) by the structured model across different impact velocities when Young's modulus of the dermal papilla is set as different values E_1=0.1 E_0, E_2=10 E_0, E_3=100 E_0, E_4=1000 E_0, where E_0=0.004MPa.

Tables

Table 1 The material properties and the element types of the paw pad used in the FE modelling of this study

Component	Element type	Young's modulus *E* (MPa)	Poisson's ratio *v*
Stratified epithelium	3D tetrahedron	6	0.495
Dermal papilla	3D tetrahedron	0.004	0.495
Top plate	3D hexahedron	-	-
Ground plate	3D hexahedron	-	-

PeerJ Preprints | https://doi.org/10.7287/peerj.preprints.2340v1 | CC BY 4.0 Open Access | rec: 4 Aug 2016, publ: 4 Aug 2016